Unsaturation in Binuclear Cyclobutadiene Iron Carbonyls: Triplet Structures, Four-Electron Bridging Carbonyl Groups, and Perpendicular Structures

Hongyan Wang,*[,†,‡] Yaoming Xie,[‡] R. Bruce King,*[,‡] and Henry F. Schaefer III[‡]

College of Sciences, Southwest Jiaotong University, Chengdu 610031, People's Republic of China, and Department of Chemistry and Center for Computational Chemistry, University of Georgia, Athens, Georgia 30602

Received December 13, 2007

In view of experimental work on $(\eta^4\text{-}C_4H_4)_2Fe_2(\mu\text{-}CO)_3$ the full range of binuclear cyclobutadieneiron carbonyls $(\eta^4\text{-}C_4H_4)_2Fe_2(CO)_n$ ($n = 5, 4, 3, 2, 1$) have been studied by density functional theory using the B3LYP and BP86 functionals. The pentacarbonyl $(\eta^4\text{-}C_4H_4)_2Fe_2(CO)_5$ is predicted to have a singly bridged $(\eta^4\text{-}C_4H_4)_2Fe_2(CO)_4(\mu\text{-}CO)$ structure with an Fe−Fe single-bond distance of 2.743 Å (BP86). For $(\eta^4\text{-}C_4H_4)_2Fe_2(CO)_4$ *cis* and *trans* doubly CO-bridged singlet structures are found as well as two types of doubly CO-bridged triplet structures. One type has Fe−Fe bond distances in the single-bond range 2.64−2.66 Å and 17-electron iron configurations. The other type of triplet structure has Fe═Fe bond distances in the range 2.38−2.39 Å for a $\sigma + {}^2/_2\pi$ double bond like that in dioxygen and 18-electron iron configurations. For $(\eta^4\text{-}C_4H_4)_2Fe_2(CO)_3$ the global minimum is the experimentally observed triply CO-bridged structure with an Fe≡Fe distance of 2.148 Å (BP86), corresponding to the triple bond required for 18-electron iron configurations. For $(\eta^4\text{-}C_4H_4)_2Fe_2(CO)_2$ the doubly CO-bridged triplet structure with an Fe≡Fe distance of 2.216 Å is the lowest energy structure. For $(\eta^4\text{-}C_4H_4)_2Fe_2(CO)$ the lowest lying singlet, triplet, and quintet structures have four-electron-donor bridging $\eta^2\text{-}\mu\text{-}CO$ groups, as indicated by Fe−O distances around 2.0−2.1 Å. Higher energy perpendicular or near-perpendicular structures with bridging C_4H_4 ligands are found in addition to coaxial structures for both $(\eta^4\text{-}C_4H_4)_2Fe_2(CO)_2$ and $(\eta^4\text{-}C_4H_4)_2Fe_2(CO)$.

1. Introduction

Unsaturated $(\eta^n\text{-}C_nR_n)_2M_2(CO)_n$ derivatives, particularly those with cyclopentadienyl or pentamethylcyclopentadienyl ligands ($n = 5$), are a source of stable compounds with metal−metal multiple bonds, particularly formal M≡M triple bonds. Such compounds date back to 1967, when King and Bisnette[1] reported the thermal reaction of pentamethylcyclopentadiene with $Mo(CO)_6$ to give $(\eta^5\text{-}Me_5C_5)_2Mo_2(CO)_4$ (Figure 1: M = Mo, R = Me). The original suggestion[1] of an Mo≡Mo triple bond in $(\eta^5\text{-}Me_5C_5)_2Mo_2(CO)_4$, based on the 18-electron rule, was later confirmed by Huang and Dahl[2] in the observation of a short Mo≡Mo distance in the crystal structure. Subsequent work indicated metal−metal triple bonds to be stable units in binuclear cyclopentadienylmetal−carbonyls of several types (Figure 1) including $(\eta^5\text{-}C_5R_5)_2V_2(CO)_5$,[3,4] $(\eta^5\text{-}C_5R_5)_2M_2(CO)_4$ (M = Cr,[5−7] Mo[1,2]), and $(\eta^5\text{-}C_5R_5)_2M'_2(CO)_3$ (M′ = Mn,[8] Re[9]). Other related compounds with formal metal−metal triple bonds include the benzene derivative[10,11] $(\eta^6\text{-}C_6H_6)_2Cr_2(\mu\text{-}CO)_3$ and the cyclobutadiene derivatives $(\eta^4\text{-}C_4R_4)_2Fe_2(\mu\text{-}CO)_3$ (R = H,[12] Me[13]). All of these metal−metal triple bonds can be assumed, at least formally, to be of the $\sigma + 2\pi$ type, similar to the C≡C triple bond in acetylene.

The situation with metal−metal double bonds in binuclear cyclopentadienylmetal carbonyls is more complicated, since structures with singlet spin states, such as $(\eta^5\text{-}C_5H_5)_2Co_2(\mu\text{-}CO)_2$,[14] and structures with triplet spin states, such as $(\eta^5\text{-}C_5H_5)_2Fe_2(\mu\text{-}CO)_3$,[15] are both known as stable compounds. In the latter triplet structure the metal−metal double bond can be considered to be a $\sigma + {}^2/_2\pi$ type, similar to the O═O double bond in O_2. An added feature of some $Cp_2M_2(CO)_n$ (Cp = $\eta^5\text{-}C_5H_5$) derivatives with M═M double bonds is their instability toward disproportionation into $Cp_2M_2(CO)_{n+1}$ with an M−M single bond and $Cp_2M_2(CO)_{n-1}$ with an M≡M triple bond. Such

* Corresponding authors. E-mail: wanghyxx@yahoo.com; rbking@chem.uga.edu.
† Southwest Jiaotong University.
‡ University of Georgia.

(1) King, R. B.; Bisnette, M. B. *J. Organomet. Chem.* **1967**, *8*, 287.
(2) Huang, J. S.; Dahl, L. F. *J. Organomet. Chem.* **1983**, *243*, 57.
(3) Cotton, F. A.; Kruczynski, L.; Frenz, B. A. *J. Organomet. Chem.* **1978**, *160*, 93.
(4) Huffman, J. C.; Lewis, L. N.; Caulton, K. G. *Inorg. Chem.* **1980**, *19*, 2755.
(5) Curtis, M. D.; Butler, W. M. *J. Organomet. Chem.* **1978**, *155*, 131.
(6) King, R. B.; Efraty, A.; Douglas, W. M. *J. Organomet. Chem.* **1973**, *60*, 125.
(7) Potenza, J.; Giordano, P.; Mastropaolo, D.; Efraty, A. *Inorg. Chem.* **1974**, *13*, 2540.
(8) Herrmann, W. A.; Serrano, R.; Weichmann, J. *J. Organomet. Chem.* **1983**, *246*, C57.
(9) Hoyano, J. K.; Graham, W. A. G. *Chem. Commun.* **1982**, 27.
(10) Knoll, L.; Riess, K.; Schaefer, J.; Kluefers, P. *J. Organomet. Chem.* **1980**, *193*, C40.
(11) Kluefers, P.; Knoll, L.; Reiners, C.; Reiss, K. *Chem. Ber.* **1985**, *118*, 1825.
(12) Fischler, I.; Hildenbrand, K.; von Gustorf, E. K. *Angew. Chem.* **1975**, *87*, 35.
(13) Herrmann, W. A.; Barnes, C. E.; Serrano, R.; Koumbouris, B. *J. Organomet. Chem.* **1983**, *256*, C30.
(14) Bailey, W. I., Jr.; Collins, D. M.; Cotton, F. A.; Baldwin, J. C. *J. Organomet. Chem.* **1979**, *165*, 373.
(15) Blaha, J. P.; Bursten, B. E.; Dewan, J. C.; Frankel, R. B.; Randolph, C. L.; Wilson, B. A.; Wrighton, M. S. *J. Am. Chem. Soc.* **1985**, *1076*, 4561.

10.1021/om701246h CCC: $40.75
Publication on Web 06/03/2008

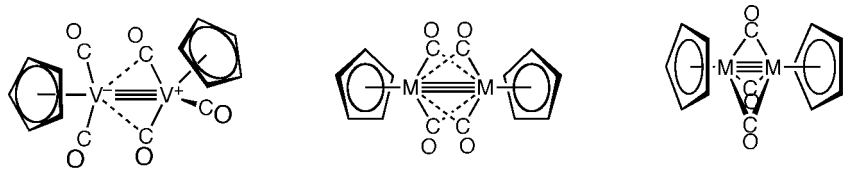

Figure 1. Some binuclear cyclopentadienylmetal carbonyl derivatives with metal−metal triple bonds.

behavior was recently observed[16] for $Cp_2Cr_2(CO)_5$ with a formal Cr═Cr double bond, which was found to disproportionate readily in solution at room temperature to $Cp_2Cr_2(CO)_6$ with a formal Cr−Cr single bond and $Cp_2Cr_2(CO)_4$ with a formal Cr≡Cr triple bond.

The binuclear cyclobutadiene iron carbonyls $(\eta^4\text{-}C_4H_4)_2Fe_2(CO)_n$ ($n = 5, 4, 3, 2, 1$) originally attracted our attention as candidates for density functional theory (DFT) studies because $(\eta^4\text{-}C_4R_4)_2Fe_2(\mu\text{-}CO)_3$ (R = H, Me), with formal Fe≡Fe triple bonds, are isolable compounds.[12,13] However, these studies led to even more interesting results for the compounds $(\eta^4\text{-}C_4H_4)_2Fe_2(CO)_4$, suggested by the 18-electron rule to contain an Fe═Fe double bond. Thus, in addition to singlet structures with Fe═Fe distances consistent with double bonds, two types of triplet structures were found for $(\eta^4\text{-}C_4H_4)_2Fe_2(CO)_4$. In one type of triplet structure of $(\eta^4\text{-}C_4H_4)_2Fe_2(CO)_4$, the triplet spin multiplicity arises from 17-electron configurations of both iron atoms. This structure has an iron−iron distance corresponding to an Fe−Fe single bond. In the other type of triplet structure of $(\eta^4\text{-}C_4H_4)_2Fe_2(CO)_4$, the iron−iron distance is appreciably shorter, consistent with an Fe═Fe double bond similar to that in the reported $(\eta^5\text{-}C_5H_5)_2Fe_2(\mu\text{-}CO)_3$ or the O═O bond in O_2. In this case both iron atoms have the favored 18-electron electronic configuration, but the Fe═Fe double bond is a $\sigma + {}^2/_2\pi$ bond with unpaired electrons in two orthogonal π orbitals. Thus the triplet structures of $(\eta^4\text{-}C_4H_4)_2Fe_2(CO)_4$ exhibit an unusual bifurcation of the iron−iron distance depending on whether the unpaired electrons reside in the π-bonding orbitals of a Fe═Fe double bond or on individual iron atoms with only an Fe−Fe single σ bond.

The more highly unsaturated $(\eta^4\text{-}C_4H_4)_2Fe_2(CO)_n$ structures also exhibit some interesting features. Thus the particular stability of Fe≡Fe triple bonds relative to double and quadruple bonds are indicated by the lower energies of triplet structures of $(\eta^4\text{-}C_4H_4)_2Fe_2(\mu\text{-}CO)_2$ with formal Fe≡Fe triple bonds and 17-electron iron configurations relative to structures with formal Fe−Fe quadruple bonds and 18-electron iron configurations. Furthermore, perpendicular structures with bridging cyclobutadiene rings as well as coaxial structures are found for $(C_4H_4)_2Fe_2(CO)_n$ ($n = 2, 1$).

2. Theoretical Methods

For carbon and oxygen the double-ζ plus polarization (DZP) basis set used here adds one set of pure spherical harmonic d functions with orbital exponents $\alpha_d(C) = 0.75$ and $\alpha_d(O) = 0.85$ to the Huzinaga−Dunning standard contracted DZ sets and is designated (9s5p1d/4s2p1d).[17,18] For H, a set of p polarization functions $\alpha_p(H) = 0.75$ is added to the Huzinaga−Dunning DZ sets. For Fe, our loosely contracted DZP basis set (14s11p6d/10s8p3d) uses Wachters' primitive set[19] augmented by two sets of p functions and one set of d functions contracted following Hood et al.[20] Thus for $(C_4H_4)_2Fe_2(CO)$, $(C_4H_4)_2Fe_2(CO)_2$, $(C_4H_4)_2Fe_2(CO)_3$, $(C_4H_4)_2Fe_2(CO)_4$, and $(C_4H_4)_2Fe_2(CO)_5$, there are 288, 318, 348, 378, and 408 contracted Gaussian functions, respectively.

Electron correlation effects were included by employing density functional theory (DFT) methods, which have evolved as a practical and effective computational tool, especially for organometallic compounds.[21−28] Two DFT methods were used in this study. The first functional is the hybrid B3LYP method, which incorporates Becke's three-parameter exchange functional (B3) with the Lee, Yang, and Parr (LYP) correlation functional.[29,30] The second approach is the BP86 method, which marries Becke's 1988 exchange functional (B) with Perdew's 1986 correlation functional.[31,32]

The geometries of all of the structures were fully optimized using both the DZP B3LYP and DZP BP86 methods. The harmonic vibrational frequencies were determined at the same levels by evaluating analytically the second derivatives of the energy with respect to the nuclear coordinates. The corresponding infrared intensities were evaluated analytically as well. The tables of ν(CO) frequencies in this paper include only the BP86 data, since previous experience shows that such frequencies are closer to the experimental values for the first-row transition metal carbonyls than ν(CO) frequencies obtained by the B3LYP method.[24] Comprehensive tables of the harmonic vibrational frequencies are given in the Supporting Information.

All of the computations were carried out with the Gaussian 94 program, in which the fine grid (75, 302) is the default for evaluating integrals numerically, and the tight (10^{-8} hartree) designation is the default for the energy convergence.[33]

In the search for minima using all currently implemented DFT methods, low-magnitude imaginary vibrational frequencies are suspect because of significant limitations in the numerical integration procedures used in the DFT computations. Thus all imaginary vibrational frequencies with a magnitude less than 100i cm^{-1} are

(16) Fortman, G. C.; Kégl, T.; Li, Q.-S.; Zhang, X.; Schaefer, H. F.; Xie, Y.; King, R. B.; Telser, J.; Hoff, C. D. *J. Am. Chem. Soc.* **2007**, *129*, 14388.
(17) Dunning, T. H. *J. Chem. Phys.* **1970**, *53*, 2823.
(18) Huzinaga, S. *J. Chem. Phys.* **1965**, *42*, 1293.
(19) Wachters, A. J. H. *J. Chem. Phys.* **1970**, *52*, 1033.
(20) Hood, D. M.; Pitzer, R. M.; Schaefer, H. F. *J. Chem. Phys.* **1979**, *71*, 705.
(21) Ehlers, A. W.; Frenking, G. *J. Am. Chem. Soc.* **1994**, *116*, 1514.
(22) Delly, B.; Wrinn, M.; Lüthi, H. P. *J. Chem. Phys.* **1994**, *100*, 5785.
(23) Li, J.; Schreckenbach, G.; Ziegler, T. *J. Am. Chem. Soc.* **1995**, *117*, 486.
(24) Jonas, V.; Thiel, W. *J. Phys. Chem.* **1995**, *102*, 8474.
(25) Barckholtz, T. A.; Bursten, B. E. *J. Am. Chem. Soc.* **1998**, *120*, 1926.
(26) Niu, S.; Hall, M. B. *Chem. Rev.* **2000**, *100*, 353.
(27) Macchi, P.; Sironi, A. *Coord. Chem. Rev.* **2003**, *238*, 383.
(28) Carreon, J.-L.; Harvey, J. N. *Phys. Chem. Chem. Phys.* **2006**, *8*, 93.
(29) Becke, A. D. *J. Chem. Phys.* **1993**, *98*, 5648.
(30) Lee, C.; Yang, W.; Parr, R. G. *Phys. Rev. B* **1988**, *37*, 785.
(31) Becke, A. D. *Phys. Rev. A* **1988**, *38*, 3098.
(32) Perdew, J. P. *Phys. Rev. B* **1986**, *33*, 8822.
(33) Frisch, M. J.; et al. *Gaussian 94, Revision B.3*; Gaussian Inc.: Pittsburgh, PA, 1995.

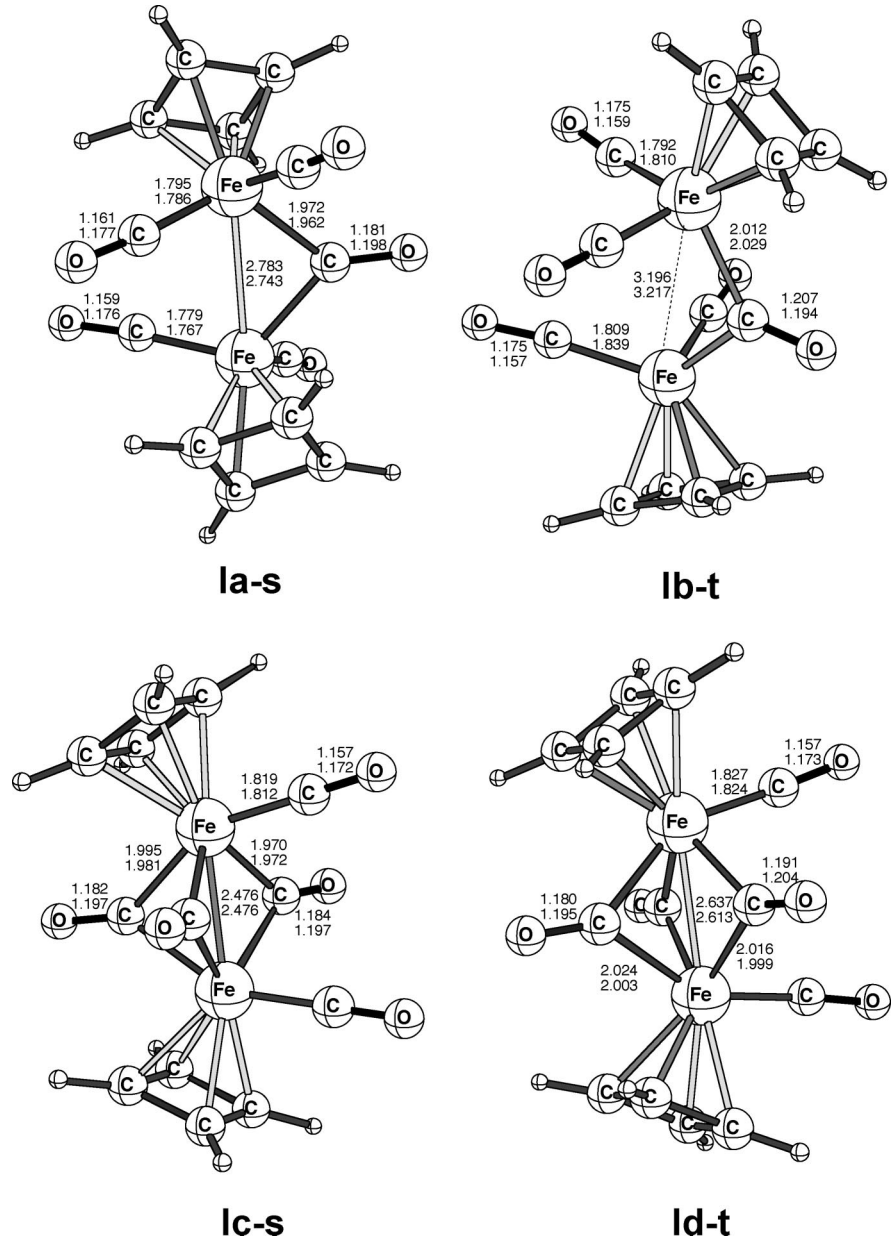

Figure 2. Optimized B3LYP (upper) and BP86 (lower) geometries for the $(C_4H_4)_2Fe_2(CO)_5$ structures (bond distances are in Å for Figures 2 to 6).

considered questionable and are given less weight in the analysis.[34–36] Therefore, we do not always follow such low imaginary vibrational frequencies.

3. Results and Discussion

3.1. Molecular Structures. 3.1.1. $(C_4H_4)_2Fe_2(CO)_5$. There are two readily imaginable structure types for singlet and triplet $(C_4H_4)_2Fe_2(CO)_5$ (Figure 2 and Tables 1 and 2), namely, the singly bridged structures $(C_4H_4)_2Fe_2(CO)_4(\mu\text{-CO})$ (**Ia-s**, **Ib-t**) and the triply bridged structures $(C_4H_4)_2Fe_2(CO)_2(\mu\text{-CO})_3$ (**Ic-s**, **Id-t**). The singlet singly bridged structure $(C_4H_4)_2Fe_2(CO)_4(\mu\text{-CO})$ (**Ia-s**) is the global minimum with all real vibrational frequencies and lies 40 kcal/mol below any of the other structures. The triplet singly bridged structure $(C_4H_4)_2Fe_2(CO)_4(\mu\text{-CO})$ (**Ib-t**) lies 39.8 kcal/mol (B3LYP) or 43.9 kcal/mol (BP86) higher and is found to have a small imaginary vibrational frequency of 12i cm^{-1} (B3LYP) or 30i cm^{-1} (BP86). The triply bridged structures $(C_4H_4)_2Fe_2(CO)_2(\mu\text{-CO})_3$ (**Ic-s**, **Id-t**) are not minima since they have large imaginary vibrational frequencies, >100i cm^{-1}. Following the largest imaginary vibrational frequency of each triply bridged structure leads to the singly bridged structures **Ia-s** and **Ib-t**, respectively.

The iron−iron bond distance for the singlet structure **Ia-s** is 2.783 Å (B3LYP) or 2.743 Å (BP86), consistent with the Fe−Fe single bond required to give both metal atoms the favored 18-electron configuration. However the iron−iron bond distance (3.196 Å/B3LYP or 3.217 Å/BP86) in the triplet structure **Ib-t** is longer than that in the corresponding monobridged singlet structures **Ia-s** by 0.41 Å/B3LYP or 0.47 Å/BP86, suggesting no significant iron−iron interaction in accord with 17-electron configurations for both iron atoms, leading to the triplet spin multiplicity. The ν(CO) frequency of the single bridging CO

(34) Jacobsen, H.; Ziegler, T. *J. Am. Chem. Soc.* **1996**, *118*, 4631.
(35) Martin, J. M. L.; Bauschlicher, C. W.; Ricca, A. *Comput. Phys. Commun.* **2001**, *133*, 189.
(36) Papas, B. N.; Schaefer, H. F. *J. Mol. Struct.* **2006**, *768*, 275.

Table 1. Bond Distances (in Å), Total Energies (*E* in hartree), and Relative Energies (Δ*E* in kcal/mol) for the $(C_4H_4)_2Fe_2(CO)_5$ Structures

	$(C_4H_4)_2Fe_2(CO)_4(\mu\text{-CO})$		$(C_4H_4)_2Fe_2(CO)_4(\mu\text{-CO})$		$(C_4H_4)_2Fe_2(CO)_2(\mu\text{-CO})_3$		$(C_4H_4)_2Fe_2(CO)_2(\mu\text{-CO})_3$	
	Ia-s (C_2)		**Ib-t** (C_2)		**Ic-s**(C_s)		**Id-t** (C_{2v})	
	B3LYP	BP86	B3LYP	BP86	B3LYP	BP86	B3LYP	BP86
Fe−Fe	2.783	2.743	3.196	3.217	2.476	2.476	2.637	2.613
Fe−C (bridge)	1.972	1.962	2.012	2.029	1.970	1.972	2.016	1.999
					1.995	1.981	2.024	2.003
C−O (bridge)	1.181	1.198	1.207	1.194	1.184	1.197	1.191	1.204
					1.182	1.197	1.180	1.195
Fe−C (terminal)	1.795	1.786	1.792	1.810	1.819	1.812	1.827	1.824
	1.779	1.767	1.809	1.839				
Fe−C (terminal)	1.161	1.177	1.175	1.159	1.157	1.172	1.157	1.173
	1.159	1.176	1.175	1.157				
−energy	3403.90853	3404.42096	3403.84510	3404.35103	3403.82187	3404.35092	3403.77235	3404.29294
Δ*E*	0.0	0.0	39.8	43.9	54.4	43.9	85.4	80.3
imaginary frequencies	none	none	12i	30i	145i, 108i	81i	236i, 173i	250i, 216i

Table 2. Metal Carbonyl *ν*(CO) Frequencies (in cm^{-1}) Predicted for the $(C_4H_4)_2Fe_2(CO)_5$ Structures (BP86) (bridging *ν*(CO) frequencies in bold; infrared intensities in km/mol are reported in parentheses)

	ν(CO) frequencies
Ia-s (C_2)	**1812(a, 382)**, 1940(b, 32), 1960(a, 1044), 1978(b, 1435), 2000(a, 16)
Ib-t (C_2)	**1735(a, 306)**, 1926(b, 361), 1946(a, 283), 1960(b, 1342) 1999(a, 747)

group appears at 1812 and 1735 cm^{-1} in the singlet **Ia-s** and triplet **Ib-t** structures, respectively (Table 2), suggesting that the Fe−Fe bond in the singlet structure reduces the Fe→CO π back-bonding to the bridging CO group.

3.1.2. $(C_4H_4)_2Fe_2(CO)_4$. Four possible singlet and triplet structures of $(C_4H_4)_2Fe_2(CO)_4$, namely, doubly bridged *cis* and *trans* structures as well as unbridged *cis* and *trans* structures, were optimized using the B3LYP and BP86 methods. A total of seven stationary points were found for $(C_4H_4)_2Fe_2(CO)_4$ after optimization, having energies within 7 kcal/mol (B3LYP) or 12 kcal/mol (BP86), indicating rather complicated potential energy surfaces (Figure 3 and Tables 3, 4, and 5). For the singlet spin state, two minima of $(C_4H_4)_2Fe_2(CO)_4$ were obtained, namely, the *trans* and *cis* doubly bridged structures **IIa-s** and **IIb-s**, respectively. The energy of the *cis* doubly bridged structure **IIb-s** is higher than that of the *trans* doubly bridged structure **IIa-s** by only 0.6 kcal/mol (B3LYP) or 1.2 kcal/mol (BP86), thus predicting a highly fluxional system. The singlet *cis/trans* unbridged structure of $(C_4H_4)_2Fe_2(CO)_4$ is not a stationary point but converts to the corresponding doubly bridged stable structure upon optimization.

Very little spin contamination was suggested for the triplet structures of $(C_4H_4)_2Fe_2(CO)_4$, as indicated by single determinant $\langle S^2 \rangle$ values close to the ideal 2.0 (Table 4). However, the results after optimization of the triplet structures are highly dependent upon the method used (B3LYP or BP86). In most cases the triplet doubly bridged structures of $(C_4H_4)_2Fe_2(CO)_4$ were found to be higher in energy than the corresponding singlet structures. The C_s *trans* doubly bridged structure **IIc-t** is predicted to have the lowest energy among the five triplet optimized structures and has all real vibrational frequencies, indicating a genuine minimum. For **IId-t** the BP86 method predicts a C_{2h} minimum. However, the B3LYP method predicts the same C_{2h} *trans* doubly bridged structure **IId-t** to lie higher in energy than the **IIc-t** by 3.7 kcal/mol with a large imaginary frequency of 222i cm^{-1}. Following the corresponding vibrational mode leads to **IIc-t**.

The *cis* doubly bridged structures all lie somewhat higher in energy than the corresponding *trans* structures. Thus, structure **IIe-t** is higher than **IIc-t** by 1.1 kcal/mol (B3LYP) or 7.7 kcal/mol (BP86), and structure **IIf-t** is higher than **IIc-t** by 5.7 kcal/mol (B3LYP) or 2.5 kcal/mol (BP86). However, **IIf-t** has a large imaginary vibrational frequency (209i cm^{-1}) by B3LYP, indicating that it is a transition state rather than a genuine minimum. Following the normal mode corresponding to the largest imaginary vibrational frequency (209i cm^{-1}) of structure **IIf-t** collapses it to **IIe-t**. The energy of the *trans* unbridged **IIg-t** is higher than that of the *trans* dibridged structure **IIc-t** by 6.6 kcal/mol (B3LYP) or 8.1 kcal/mol (BP86). However, the *trans* unbridged structure is found to have small imaginary vibrational frequencies of 49i and 16i cm^{-1} (B3LYP) or 66i cm^{-1} (BP86). Following the corresponding normal modes converts **IIg-t** to **IIc-t**.

Six of the seven $(\eta^4\text{-}C_4H_4)_2Fe_2(CO)_4$ structures in Figure 3 have two bridging carbonyl groups. The predicted *ν*(CO) frequencies for these two bridging carbonyl groups fall in the fairly typical range 1800 to 1847 cm^{-1}, which is more than 100 cm^{-1} below the terminal *ν*(CO) frequencies for the same compounds.

The Fe═Fe distances predicted for the singlet doubly bridged structures $(\eta^4\text{-}C_4H_4)_2Fe_2(CO)_2(\mu\text{-CO})_2$, namely, **IIa-s** and **IIb-s**, fall in the range 2.61 to 2.65 Å. Similar Fe−Fe distances were found in the triplet doubly bridged **IIe-t**. However, the significantly shorter predicted Fe═Fe bond distance of 2.388 Å (B3LYP) or 2.386 Å (BP86) for the likewise triplet doubly bridged structures **IId-t** and **IIf-t** can be interpreted as a $\sigma + {}^2/_2\pi$ double bond. Such a bonding arrangement is similar to the Fe═Fe double bond in the triplet triply bridged structure $(\eta^5\text{-}Me_5C_5)_2Fe_2(\mu\text{-CO})_3$, shown by X-ray diffraction[15] to have an iron−iron distance of 2.265 Å. Thus two distinctly different types of triplet structures are predicted for $(\eta^4\text{-}C_4H_4)_2Fe_2(CO)_4$. In **IIe-t** the Fe−Fe distance corresponds to a single bond, leading to a 17-electron configuration for each iron atom and thus an unpaired electron on each iron atom. However, in **IId-t** and **IIf-t** the Fe═Fe distances correspond to double bonds, leading to an 18-electron configuration for each iron atom. In these cases the two unpaired electrons of the triplet are in the π orbitals of the $\sigma + {}^2/_2\pi$ double bond.

3.1.3. $(C_4H_4)_2Fe_2(CO)_3$. Structures of $(C_4H_4)_2Fe_2(CO)_3$ having three, two, or one bridging CO groups have been examined (Figure 4 and Tables 6 and 7). The singly and doubly bridged singlet stationary points of $(C_4H_4)_2Fe_2(CO)_3$ collapse to the triply bridged structure $(C_4H_4)_2Fe_2(\mu\text{-CO})_3$ (**IIIa-s**), which appears to be the global minimum without any imaginary frequencies.

The singly bridged triplet structure $(C_4H_4)_2Fe_2(CO)_2(\mu\text{-CO})$ collapses to the triply bridged $(C_4H_4)_2Fe_2(\mu\text{-CO})_3$ (**IIIc-t**), which is a transition state with the large imaginary vibrational frequencies 435i cm^{-1} (B3LYP) or 721i cm^{-1} and 423i cm^{-1} (BP86). Following the 435i cm^{-1} (B3LYP) or 721i cm^{-1} (BP86)

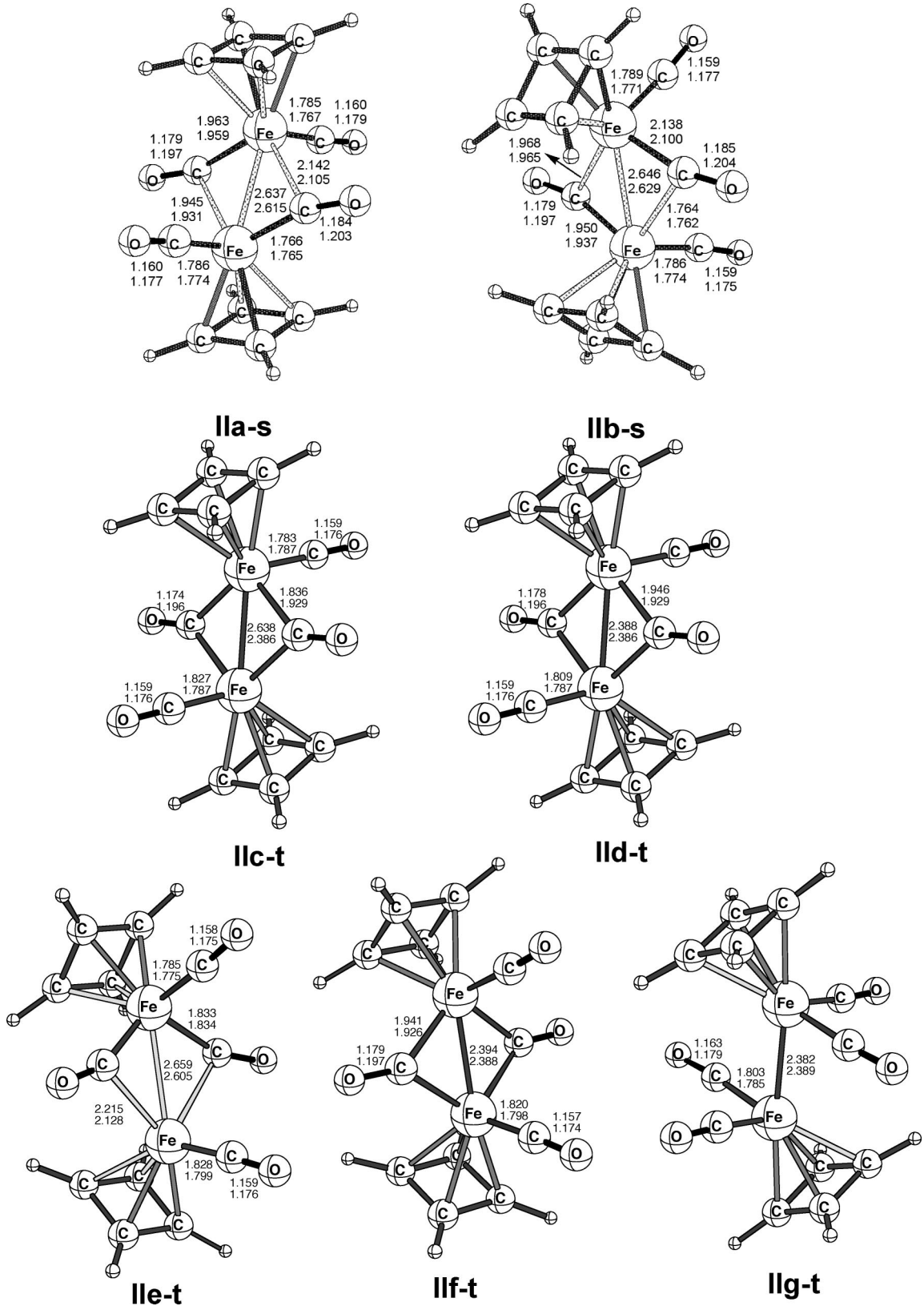

Figure 3. Optimized B3LYP (upper) and BP86 (lower) geometries for the $(C_4H_4)_2Fe_2(CO)_4$ structures.

imaginary frequency leads to the doubly bridged structure $(C_4H_4)_2Fe_2(CO)(\mu\text{-}CO)_2$ (**IIIb-t**), which is found to be a genuine minimum without imaginary frequencies. The doubly bridged triplet structure (**IIIb-t**) lies 8.6 kcal/mol (B3LYP) or 24.5 kcal/mol (BP86) above the singlet global minimum **IIIa-s**.

The three ν(CO) frequencies for the triply bridged singlet $(C_4H_4)_2Fe_2(\mu\text{-}CO)_3$ structure **IIIa-s** fall in the range 1854−1888 cm^{-1} (Table 7), which is appreciably higher than the 1813 and 1824 cm^{-1} bridging ν(CO) frequencies for the doubly bridged triplet $(C_4H_4)_2Fe_2(CO)(\mu\text{-}CO)_2$. This suggests stronger Fe→CO π back-bonding in the triplet state relative to the singlet.

The Fe≡Fe bond distance for the triply bridged singlet $(C_4H_4)_2Fe_2(\mu\text{-}CO)_3$ structure **IIIa-s** is 2.147 Å (B3LYP) or 2.148 Å (BP86), consistent with the triple bond required to give each

Table 3. Bond Distances (in Å), Total Energies (*E* in hartree), and Relative Energies (Δ*E* in kcal/mol) for the Singlet $(C_4H_4)_2Fe_2(CO)_4$ Structures

	trans-$(C_4H_4)_2Fe_2(CO)_2(\mu\text{-}CO)_2$		*cis*-$(C_4H_4)_2Fe_2(CO)_2(\mu\text{-}CO)_2$	
	IIa-s (C_1)		**IIb-s** (C_1)	
	B3LYP	BP86	B3LYP	BP86
Fe−Fe	2.637	2.615	2.646	2.629
Fe−C(bridge)	1.963/2.142	1.959/2.159	1.968/2.138	1.965/2.100
	1.945/1.766	1.931/1.765	1.950/1.764	1.937/1.762
Fe−C(terminal)	1.785/1.786	1.767/1.774	1.789/1.786	1.771/1.774
C−O(bridge)	1.179/1.184	1.197/1.203	1.179/1.185	1.197/1.204
C−O(terminal)	1.160/1.160	1.177/1.179	1.159/1.159	1.177/1.175
−energy	3290.52529	3291.03140	3290.52439	3291.02955
Δ*E*	0.0	0.0	0.6	1.2
imaginary frequencies	none	none	none	none

Table 4. Bond Distances (in Å), Total Energies (*E* in hartree), Relative Energies (Δ*E* in kcal/mol), and Spin Contamination $\langle S^2\rangle$ for the triplet $(C_4H_4)_2Fe_2(CO)_4$ Structures

		trans-$(C_4H_4)_2Fe_2(CO)_2(\mu\text{-}CO)_2$		*cis*-$(C_4H_4)_2Fe_2(CO)_2(\mu\text{-}CO)_2$		*trans*- $(C_4H_4)_2Fe_2(CO)_4$
		IIc-t (C_s)	**IId-t** (C_{2h})	**IIe-t** (C_s)	**IIf-t** (C_{2v})	**IIg-t** (C_{2h})
Fe−Fe	B3LYP	2.638	2.388	2.659	2.394	2.382
	BP86	2.386	2.386	2.605	2.388	2.389
−*E*	B3LYP	3290.52523	3290.51934	3290.52345	3290.51620	3290.51478
	BP86	3291.02403	3291.02403	3291.01177	3291.02004	3291.01106
Δ*E*	B3LYP	0.04	3.7	1.2	5.7	6.6
	BP86	4.6	4.6	12.3	7.1	12.8
imaginary	B3LYP	none	222i	28i	209i, 62i	49i, 16i
frequencies	BP86	none	none	none	none	66i
$\langle S^2\rangle$	B3LYP	2.10	2.10	2.09	2.12	2.20
	BP86	2.01	2.01	2.02	2.02	2.04

Table 5. Metal Carbonyl *ν*(CO) Frequencies (in cm^{-1}) Predicted for the $(C_4H_4)_2Fe_2(CO)_4$ Structures (BP86) (bridging *ν*(CO) frequencies in bold; symmetries and infrared intensities in km/mol are given in parentheses)

	ν(CO) frequencies
IIa-s (C_1)	**1802(a, 513), 1826(a, 204),** 1955(a, 1295) 1973(a, 187)
IIb-s (C_1)	**1800(a, 497), 1826(a, 224),** 1961(a, 398), 1991(a, 1152)
IIc-t (C_s)	**1822(a″, 935), 1825(a′, 0)**, 1955(a′, 1548), 972(a′, 0)
IId-t (C_{2h})	**1822(a_u, 936), 1825(a_g, 0),** 1955(b_u, 1546), 1972(a_g, 0)
IIe-t (C_s)	**1833(a″, 807), 1847(a′, 8),** 1955(a′, 488), 1990(a′, 1177)
IIf-t (C_{2v})	**1816(b1, 917), 1820(a1, 27**), 1954(b_2, 369), 1991(a_1, 1214)
IIg-t (C_{2h})	1936(b_u, 1148), 1926(b_g, 0), 1981(a_g, 0), 1945(a_u, 1315)

iron atom the favored 18-electron configuration. However the Fe═Fe bond distance in the triplet **IIIb-t** (2.363 Å by B3LYP or 2.309 Å by BP86) is significantly longer than that for **IIIa-s**, consistent with the double bond needed to give each iron atom the 17-electron configuration corresponding to triplet spin multiplicity.

Both $(\eta^4\text{-}C_4H_4)_2Fe_2(CO)_3$[12] and $(\eta^4\text{-}Me_4C_4)_2Fe_2(CO)_3$[13] have been reported in the literature, but without any definitive structural information by X-ray diffraction for either compound. The permethylated derivative $(\eta^4\text{-}Me_4C_4)_2Fe_2(CO)_3$ is described as shiny red needles with correct C, H, and Fe analyses and a single infrared *ν*(CO) frequency at 1829 cm^{-1} in hexane.[12] This experimental *ν*(CO) frequency agrees well with the presumably unresolvable pair of infrared *ν*(CO) frequencies at 1854 and 1855 cm^{-1} predicted for the triply bridged global minimum structure **IIIa-s** (Table 7 and Figure 4). Note that the substitution of methyl groups for hydrogen atoms leads to increased *π* back-

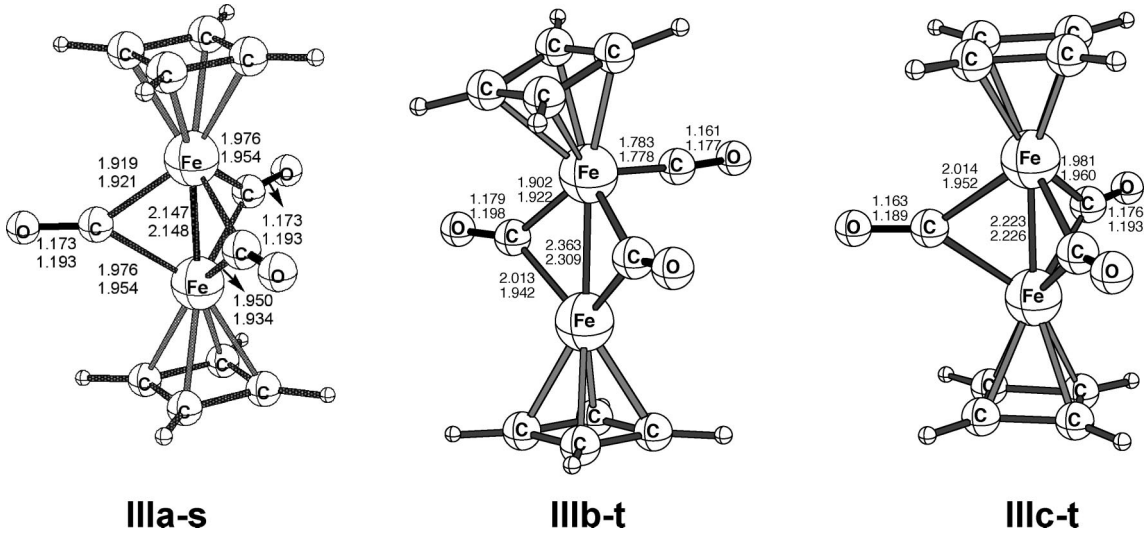

Figure 4. Optimized B3LYP (upper) and BP86 (lower) geometries for the $(C_4H_4)_2Fe_2(CO)_3$ structures.

Table 6. Bond Distances (in Å), Total Energies (*E* in hartree), Relative Energies (Δ*E* in kcal/mol), and Spin Contamination $\langle S^2 \rangle$ for the $(C_4H_4)_2Fe_2(CO)_3$ Stationary Points

	$(C_4H_4)_2Fe_2(\mu\text{-}CO)_3$		$(C_4H_4)_2Fe_2(CO)\ (\mu\text{-}CO)_2$		$(C_4H_4)_2Fe_2(\mu\text{-}CO)_3$	
	IIIa-s (C_{2v})		**IIIb-t** (C_s)		**IIIc-t** (C_{2v})	
	B3LYP	BP86	B3LYP	BP86	B3LYP	BP86
Fe−Fe	2.147	2.148	2.363	2.309	2.223	2.226
Fe−C(bridge)	1.919/1.976 /1.950	1.921/1.954 /1.934	1.902/2.013	1.922/1.942	1.981/2.014	1.960/1.952
Fe−C(terminal)			1.783	1.778		
C−O(bridge)	1.173	1.193	1.179	1.198	1.163/1.176	1.189/1.193
C−O(terminal)			1.161	1.177		
−energy	3177.16281	3177.67216	3177.14896	3177.63298	3177.11523	3177.61312
Δ*E*	0.0	0.0	8.7	24.6	29.9	37.1
imaginary frequencies	none	none	none	none	435i	721i, 423i
$\langle S^2 \rangle$	0.00	0.00	2.23	2.03	2.42	2.05

Table 7. Metal Carbonyl *ν*(CO) Frequencies (in cm^{-1}) Predicted for the $(C_4H_4)_2Fe_2(CO)_3$ Structures (BP86) (bridging *ν*(CO) frequencies in bold)

	ν(CO) frequencies
IIIa-s (C_2)	**1855(a, 876), 1854(b, 912), 1888(a, 0)**
IIIb-t(C_s)	**1813(a″, 996), 1824(a′, 85),** 1967(a′, 697)

bonding from the metal to the carbonyl groups, thereby lowering the effective CO bond order and the corresponding *ν*(CO) frequencies.

Interpretation of the reported[12] experimental *ν*(CO) frequencies for the unsubstituted $(\eta^4\text{-}C_4H_4)_2Fe_2(CO)_3$ is more complicated. Thus the photolysis of $(\eta^4\text{-}C_4H_4)Fe(CO)_3$ in tetrahydrofuran at −40 °C is reported to give an extremely sensitive dark red product exhibiting strong terminal *ν*(CO) frequencies at 1980 and 2051 cm^{-1} and a strong bridging *ν*(CO) frequency at 1861 cm^{-1}. The observed terminal *ν*(CO) frequencies do not correspond to those predicted for any of the binuclear $(\eta^4\text{-}C_4H_4)_2Fe_2(CO)_n$ derivatives discussed in this paper. However, they correspond very closely to the reported[37] *ν*(CO) frequencies of 1985 and 2055 cm^{-1} for $(\eta^4\text{-}C_4H_4)Fe(CO)_3$, which could be unreacted starting material and/or arise from decomposition of the extremely sensitive dark red product. This leaves only the bridging *ν*(CO) frequency at 1861 cm^{-1} for the dark red product itself, which is remarkably close to the predicted pair of infrared

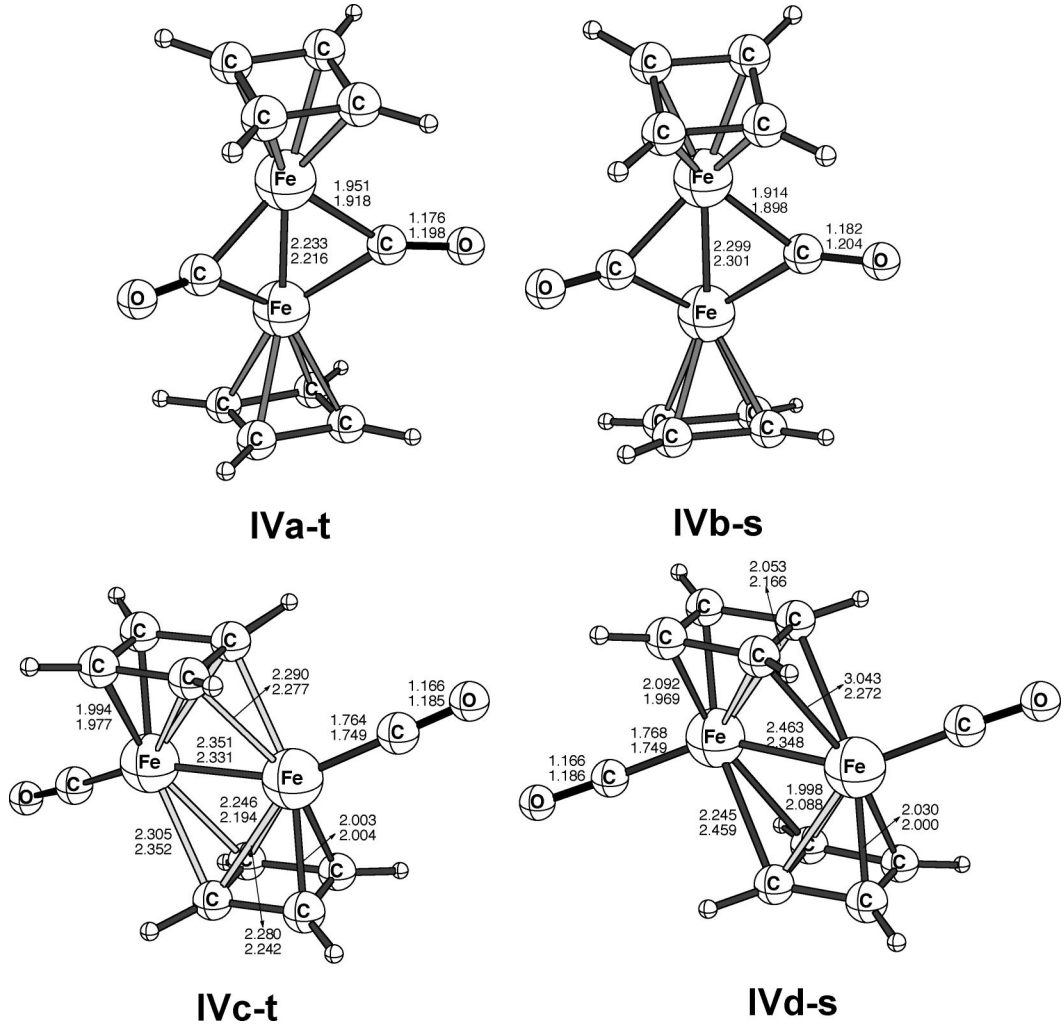

Figure 5. Optimized B3LYP (upper) and BP86 (lower) geometries for the $(C_4H_4)_2Fe_2(CO)_2$ structures.

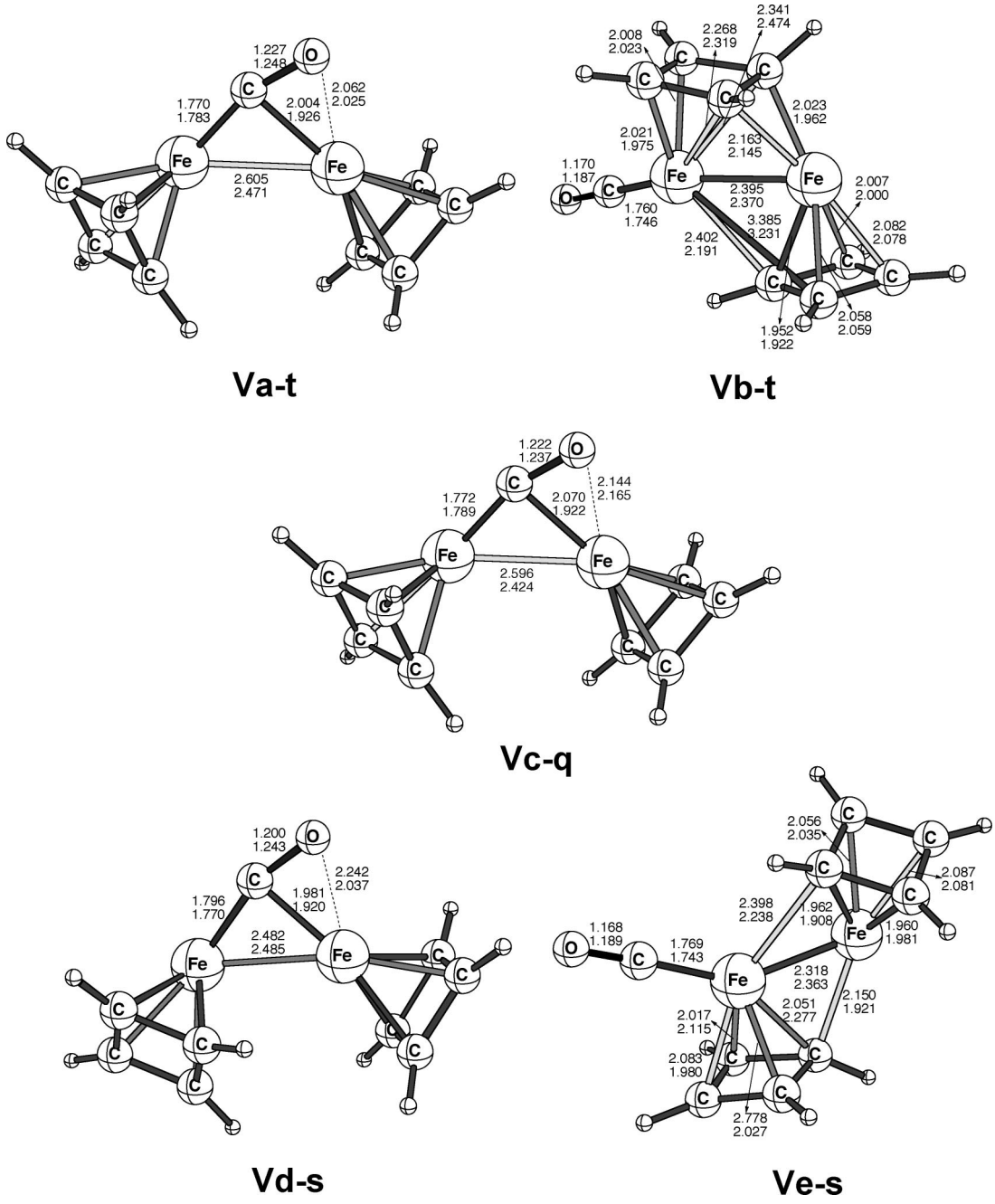

Figure 6. Optimized B3LYP (upper) and BP86 (lower) geometries for the $(C_4H_4)_2Fe_2(CO)$ structures.

ν(CO) frequencies at 1854 and 1855 cm^{-1} for the triply CO-bridged global minimum **IIIa-s** (Figure 4), which are not resolved under the experimental conditions.

The authors of the 1975 report[12] on the photolysis of (η^4-C_4H_4)$Fe(CO)_3$ to give (η^4-C_4H_4)$_2Fe_2(CO)_3$ interpret the three observed ν(CO) frequencies of 1861, 1985, and 2055 cm^{-1} as indicating a singly bridged structure (η^4-C_4H_4)$_2Fe_2(CO)_2$(μ-CO) for their dark red product. Since we do not find a structure of this type in our DFT studies of (η^4-C_4H_4)$_2Fe_2(CO)_3$, we suggest reinterpretation of their reported spectrum[12] as indicating a triply carbonyl bridged structure (η^4-C_4H_4)$_2Fe_2(\mu$-CO)$_3$, which we find as the global minimum **IIIa-s** (Figure 4), contaminated with (η^4-C_4H_4)$Fe(CO)_3$, as unreacted starting material and/or a decomposition product of (η^4-C_4H_4)$_2Fe_2(\mu$-CO)$_3$.

3.1.4. $(C_4H_4)_2Fe_2(CO)_2$. There are two types of stationary points for $(C_4H_4)_2Fe_2(CO)_2$, namely, coaxial and perpendicular structures, for both the singlet and triplet spin states (Figure 5 and Tables 8, 9, and 10). In contrast to $(C_4H_4)_2Fe_2(CO)_n$ (n = 5, 4, 3) discussed above, the energies of the triplet $(C_4H_4)_2Fe_2(CO)_2$ structure are lower than those of the singlet structures (Table 8). Thus the predicted global minimum for $(C_4H_4)_2Fe_2(CO)_2$ is the triplet C_{2v} structure **IVa-t** with two symmetrical bridging CO ligands.

The lowest energy singlet and triplet stationary points of $(C_4H_4)_2Fe_2(CO)_2$, namely, **IVa-t** and **IVb-s**, respectively, have coaxial structures, $(C_4H_4)_2Fe_2(\mu$-$CO)_2$, with two bridging CO groups. The other two structures for $(C_4H_4)_2Fe_2(CO)_2$ found in this work, namely, triplet **IVc-t** and singlet **IVd-s**, have perpendicular dimetallocene structures with two terminal CO groups similar to that computed for the carbonyl-free dimetallocenes Cp_2M_2 (M = Cu, Ni)[38] and perpendicular $\perp$-Cp_2-

(37) Emerson, G. F.; Watts, L.; Pettit, R. *J. Am. Chem. Soc.* **1965**, *87*, 132.

Table 8. Bond Distances (in Å), Total Energies (*E* in hartree), Relative Energies (Δ*E* in kcal/mol), and Spin Contamination $\langle S^2 \rangle$ for the Triplet State $(C_4H_4)_2Fe_2(CO)_2$ Structures

	$(C_4H_4)_2Fe_2(CO)_2$		$(C_4H_4)_2Fe_2(CO)(\mu\text{-}CO)$	
	IVa-t (C_{2v})		**IVc-t** (C_2)	
	B3LYP	BP86	B3LYP	BP86
Fe−Fe	2.233	2.216	2.351	2.331
Fe−C(bridge)	1.951	1.918		
Fe−C (terminal)			1.764	1.749
C−O(bridge)	1.176	1.198	1.166	1.185
C−O(terminal)				
−energy	3063.76700	3064.23717	3063.74373	3064.20028
Δ*E*	0.0	0.0	14.6	23.1
imaginary frequencies	none	none	none	none
$\langle S^2 \rangle$	2.34	2.06	2.13	2.05

Table 9. Bond Distances (in Å), Total Energies (*E* in Hartree), and Relative Energies (Δ*E* in kcal/mol) for the Singlet State $(C_4H_4)_2Fe_2(CO)_2$ Structures

	$(C_4H_4)_2Fe_2(\mu\text{-}CO)_2$		$(C_4H_4)_2Fe_2(CO)(\mu\text{-}CO)$	
	IVb-s (C_{2v})		**IVd-s** (C_i)	
	B3LYP	BP86	B3LYP	BP86
Fe−Fe	2.299	2.301	2.463	2.348
Fe−C(bridge)	1.914	1.898		
Fe−C (terminal)			1.768	1.749
C−O(bridge)	1.182	1.204		
C−O(terminal)			1.166	1.186
−energy	3063.73192	3064.22496	3063.72699	3064.18788
Δ*E*	22.0	7.7	25.1	30.9
imaginary frequencies	none	none	37i	24i

Table 10. Metal Carbonyl ν(CO) Frequencies (in cm^{-1}) Predicted for the $(C_4H_4)_2Fe_2(CO)_2$ Structures (BP86) (bridging ν(CO) frequencies in bold; infrared intensities in km/mol are in parentheses)

	ν(CO) frequencies
IVa-t (C_{2v})	**1825(b_2,1013), 1838(a_1, 68)**
IVb-s (C_{2v})	**1789(b_2, 839), 1806(a_1, 75)**
IVc-t (C_2)	1918(b, 2221), 1936(a, 38)
IVd-s (C_i)	1911(a_u, 2402),1934(a_g, 0)

$Co_2(CO)_2$..[39] In both **IVc-t** and **IVd-s** two carbon atoms of each cyclobutadiene ring bridge the iron−iron bond. The doubly CO-bridged coaxial structures **IVa-t** and **IVb-s** lie lower in energy than the perpendicular structures of corresponding multiplicities **IVc-t** and **IVd-s**, respectively, by 14.6 and 3.1 kcal/mol (B3LYP) or 23.1 and 23.2 kcal/mol (BP86), respectively.

The theoretical iron−iron distance in **IVa-t** is only 2.233 Å (B3LYP) or 2.216 Å (B3LYP), consistent with the Fe≡Fe triple bond required to give each iron atom in **IVa-t** the 17-electron rare gas configuration for a molecular triplet spin state. The Fe−Fe distance in the singlet doubly CO-bridged structure **IVb-s** is 2.299 Å (B3LYP) or 2.301 Å (BP86). This should correspond to the quadruple bond to give the iron atoms 18-electron configurations, but unexpectedly is ∼0.066 Å (B3LYP) or 0.085 Å (BP86) longer than the Fe≡Fe distance in the triplet doubly CO-bridged structure **IVa-t**. The iron−iron distance in the triplet perpendicular structure **IVc-t** at 2.351 Å (B3LYP) or 2.331 Å (BP86) is ∼0.11 Å (B3LYP) or 0.02 Å (BP86) shorter than the iron−iron distance in the singlet perpendicular structure **IVd-s** at 2.463 Å (B3LYP) or 2.348 Å (BP86).

3.1.4. $(C_4H_4)_2Fe_2(CO)$. Optimizations have been carried out on triplet and singlet $(C_4H_4)_2Fe_2(CO)$ structures in which the single CO group is either bridging or terminal. Since considerable spin contamination was found for the triplet structures, particularly when using the B3LYP method (Table 11), a quintet structure for $(C_4H_4)_2Fe_2(CO)$ was also optimized.

Two types of minima are obtained for $(C_4H_4)_2Fe_2(CO)$ (Figure 6 and Table 11). One type is the *cisoid* dimetallocene structure with a bridging CO ligand (**Va-t**, **Vc-q**, and **Vd-s**). These dimetallocenes have bent structures because of their single η^2-μ-CO bridge. This bridging η^2-μ-CO group in all three structures can be considered to be a formal four-electron donor to the pair of metal atoms, since it bonds to one of the metal atoms as a normal two-electron donor linear CO ligand and to the other metal atom through an electron pair from a C−O π bond. Such four-electron donor CO groups are characterized by unusually short Fe−O distances (Figure 6) and unusually low ν(CO) frequencies (Table 11). Thus, the Fe−O distances are 2.062 Å (B3LYP) or 2.025 Å (BP86) in **Va-t**, 2.144 Å (B3LYP) or 2.165 Å (BP86) in **Vc-q**, and 2.242 Å (B3LYP) or 2.037 Å (BP86) in **Vd-s**.

The very low ν(CO) frequencies for these $(C_4H_4)_2Fe_2(\mu\text{-}CO)$ derivatives (BP86) are 1581 cm^{-1} in **Va-t**, 1631 cm^{-1} in **Vc-q**, and 1615 cm^{-1} in **Vd-s**. The iron−iron distances (Table 11) are similar (2.61 to 2.48 Å) for all three dimetallocene $(C_4H_4)_2Fe_2(\mu\text{-}CO)$ structures (**Va-t**, **Vc-q**, and **Vd-s**) regardless of their spin multiplicities.

The other structures for $(\mu\text{-}C_4H_4)_2Fe_2(CO)$, namely, **Vb-t** and **Ve-s**, are perpendicular dimetallocene structures[38] with the metal−metal bond axis parallel or nearly parallel to the cyclobutadiene rings and a terminal CO ligand bonded to one of the metal atoms. In structures **Vb-t** and **Ve-s**, each C_4H_4 ring bridges the two iron atoms, in contrast to structures **Va-t** and **Vd-s**, in which the C_4H_4 rings are each bonded to only a single iron atom as tetrahapto ligands.

3.2. Comparison of the Structures of $(C_4H_4)_2Fe_2(CO)_n$ and $(C_5H_5)_2Mn_2(CO)_n$ (n = 5, 4, 3, 2, and 1). Table 12 compares the global minimum structures found in this work for $(C_4H_4)_2Fe_2(CO)_n$ with those found in previous work[40] for the isoelectronic $(C_5H_5)_2Mn_2(CO)_n$ (n = 5, 4, 3, and 2) using the BP86 method. Table 12 also includes the formal metal−metal bond orders assuming 18-electron metal configurations for the singlets (n = 5, 4, and 3) and 17-electron metal configurations for the dicarbonyl triplets (n = 2).

The isoelectronic $(C_4H_4)_2Fe_2(CO)_n$ and $(C_5H_5)_2Mn_2(CO)_n$ (n = 5, 4, 3, and 2) have analogous global minimum structures, except that the perpendicular metallocenes were not found for $(C_5H_5)_2Mn_2(CO)_2$. Each unit increase in the formal metal−metal bond order is predicted to shorten the Fe−Fe bond distances (BP86) by roughly 0.3 Å, in accord with the theoretical structures[40] of $(C_5H_5)_2Mn_2(CO)_n$ (n = 5, 4, 3, and 2).

There are some difficulties with the interpretation of the iron−iron bond as an Fe−Fe quadruple bond in the structures **IVb-s** and **Vd-s**. Thus the relatively long Fe−Fe distance of 2.299 Å (B3LYP) or 2.301 Å (BP86) in the singlet structure **IVb-s** and 2.482 Å (B3LYP) or 2.485 Å (BP86) in the singlet structure **Vd-s** are inconsistent with the quadruple bond

(38) Xie, Y.; Schaefer, H. F.; King, R. B. *J. Am. Chem. Soc.* **2005**, *127*, 2818.

(39) Wang, H.; Xie, Y.; King, R. B.; Schaefer, H. F. *J. Am. Chem. Soc.* **2005**, *127*, 11564.

(40) Li, Q.-S.; Zhang, X.; Xie, Y.; King, R. B.; Schaefer, H. F. *Organometallics* **2008**, *27*, 61.

Table 11. Bond Distances (in Å), Total Energies (*E* in hartree), Relative Energies (Δ*E* in kcal/mol), and Spin Contamination $\langle S^2 \rangle$ for the $(C_4H_4)_2Fe_2(CO)$ Structures

	$(C_4H_4)_2Fe_2(\mu\text{-CO})$		$(C_4H_4)_2Fe_2(CO)$		$(C_4H_4)_2Fe_2(\mu\text{-CO})$		$(C_4H_4)_2Fe_2(\mu\text{-CO})$		$(C_4H_4)_2Fe_2(CO)$	
	Va-t (C_1)		**Vb-t** (C_1)		**Vc-q** (C_1)		**Vd-s** (C_1)		**Ve-s** (C_1)	
	B3LYP	BP86	B3LYP	BP86	B3LYP	BP86	B3LYP	BP86	B3LYP	BP86
Fe−Fe	2.605	2.471	2.395	2.370	2.596	2.424	2.482	2.485	2.318	2.363
Fe−C(b)	1.770 2.004	1.783 1.926			1.772 2.070	1.789 1.922	1.796 1.981	1.770 1.920		
C−O(b)	1.227	1.248			1.222	1.237	1.200	1.243		
Fe−C(t)			1.760	1.746					1.769	1.743
Fe−C(t)			1.170	1.187					1.168	1.189
−energy	2950.35757	2950.79536	2950.35177	2950.79522	2950.35140	2950.78976	2950.30814	2950.77600	2950.32003	2950.77751
Δ*E*	0.0	0.0	3.6	0.1	3.9	3.5	31.0	12.1	23.6	11.2
imaginary frequencies	none	none	none	none	none	none	none	none	none	none
ν(CO), cm^{-1}	1684	1581	2000	1915	1702	1631	1801	1615	2012	1909
$\langle S^2 \rangle$	2.60	2.25	2.27	2.07	6.52	6.11	0.00	0.00	0.00	0.00

Table 12. Comparison of the Metal−Metal Distances (in Å) and Formal Metal−Metal Bond Orders for the Global Minima of $(C_4H_4)_2Fe_2(CO)_n$ and $(C_5H_5)_2Mn_2(CO)_n$ (n = 5, 4, 3, and 2)

	structure	symmetry	no. of bridging COs	M-M	M-C	C−O	formal M−M bond order
$(C_4H_4)_2Fe_2(CO)_5$	**Ia-s**	C_2	1	2.743	1.962	1.198	1
$(C_5H_5)_2Mn_2(CO)_5$	**5S-1**	C_2	1	2.804	1.982	1.203	1
$(C_4H_4)_2Fe_2(CO)_4$	**IIa-s**	C_i	2	2.615	1.954/1.771	1.189	2
$(C_5H_5)_2Mn_2(CO)_4$	**4S-1**	C_i	2	2.509	1.795/2.278	1.194	2
$(C_4H_4)_2Fe_2(CO)_3$	**IIIa-s**	C_s	3	2.148	1.936	1.193	3
$(C_5H_5)_2Mn_2(CO)_3$	**3S-1**	C_2	3	2.167	1.941/1.947	1.201	3
$(C_4H_4)_2Fe_2(CO)_2$	**IVa-t**	C_{2v}	2	2.216	1.918	1.198	3
$(C_5H_5)_2Mn_2(CO)_2$	**2T-1**	C_{2v}	2	2.202	1.926	1.205	3

Table 13. Dissociation Energies (kcal/mol) for the Successive Removal of Carbonyl Groups from $(C_4H_4)_2Fe_2(CO)_n$ and $(C_5H_5)_2Mn_2(CO)_n$ Derivatives

	B3LYP	BP86
$(C_4H_4)_2Fe_2(CO)_5$ (**Ia-s**) → $(C_4H_4)_2Fe_2(CO)_4$ (**IIa-s**) + CO	34.2	39.1
$(C_4H_4)_2Fe_2(CO)_4$ (**IIa-s**) → $(C_4H_4)_2Fe_2(CO)_3$ (**IIIa-s**) + CO	21.2	20.1
$(C_4H_4)_2Fe_2(CO)_3$ (**IIIa-s**) → $(C_4H_4)_2Fe_2(CO)_2$ (**IVa-t**) + CO	42.1	67.5
$(C_4H_4)_2Fe_2(CO)_2$ (**IVa-t**) → $(C_4H_4)_2Fe_2(CO)$ (**Va-t**) +CO	50.7	71.9
$(C_5H_5)_2Mn_2(CO)_5$ (**5s-1**) → $(C_5H_5)_2Mn_2(CO)_4$ (**4s-1**) + CO	34.1	42.4
$(C_5H_5)_2Mn_2(CO)_4$ (**4s-1**) → $(C_5H_5)_2Mn_2(CO)_3$ (**3s-1**) + CO	16.2	15.5
$(C_5H_5)_2Mn_2(CO)_3$ (**3s-1**)→ $(C_5H_5)_2Mn_2(CO)_2$ (**2T-1**) + CO	46.4	67.0

Table 14. Energies (kcal/mol) for the Disproportionation Reaction $2(C_4H_4)_2Fe_2(CO)_n \rightarrow (C_4H_4)_2Fe_2(CO)_{n+1} + (C_4H_4)_2Fe_2(CO)_{n-1}$

	B3LYP	BP86
$2(C_4H_4)_2Fe_2(CO)_4$ (**IIa-s**) → $(C_4H_4)_2Fe_2(CO)_5$ (**Ia-s**) + $(C_4H_4)_2Fe_2(CO)_3$ (**IIIa-s**)	−13.0	−19.0
$2(C_4H_4)_2Fe_2(CO)_3$ (**IIIa-s**) → $(C_4H_4)_2Fe_2(CO)_4$ (**IIa-s**) + $(C_4H_4)_2Fe_2(CO)_2$ (**IVa-t**)	20.9	47.5
$2(C_4H_4)_2Fe_2(CO)_2$ (**IVa-t**) → $(C_4H_4)_2Fe_2(CO)_3$ (**IIIa-s**) + $(C_4H_4)_2Fe_2(CO)$ (**Va-t**)	8.5	4.3
$2(C_5H_5)_2Mn_2(CO)_4$ → $(C_5H_5)_2Mn_2(CO)_5$ + $(C_5H_5)_2Mn_2(CO)_3$	−17.9	−27.0
$2(C_5H_5)_2Mn_2(CO)_3$ → $(C_5H_5)_2Mn_2(CO)_4$ + $(C_5H_5)_2Mn_2(CO)_2$	30.1	51.6

required to give both metal atoms the favored 18-electron configuration. They more likely correspond to Fe═Fe double bonds to give the metal atoms 16-electron configurations.

3.3. Dissociation Energies. Table 13 reports the dissociation energies of the single carbonyl dissociation steps

$$(C_4H_4)_2Fe_2(CO)_n \rightarrow (C_4H_4)_2Fe_2(CO)_{n-1} + CO$$

In determining these dissociation energies, the fragments were allowed to relax.

The predicted energy of 21.2 kcal/mol (B3LYP) or 20.1 kcal/mol (BP86) for the dissociation of one CO group from $(C_4H_4)_2Fe_2(CO)_4$ to give $(C_4H_4)_2Fe_2(CO)_3$ is much less than the predicted dissociation energies of one CO group from $(C_4H_4)_2Fe_2(CO)_5$ to give $(C_4H_4)_2Fe_2(CO)_4$ or from $(C_4H_4)_2Fe_2(CO)_3$ to give $(C_4H_4)_2Fe_2(CO)_2$. Both $(C_4H_4)_2Fe_2(CO)_3$ and $(C_4H_4)_2Fe_2(CO)_2$ appear to be very stable with respect to dissociation of a carbonyl ligand. This behavior is similar to that of the corresponding $(C_5H_5)_2Mn_2(CO)_n$ derivatives.[40]

Table 14 lists the energies for the following disproportionation reactions:

$$2(C_4H_4)_2Fe_2(CO)_n \rightarrow (C_4H_4)_2Fe_2(CO)_{n+1} + (C_4H_4)_2Fe_2(CO)_{n-1}$$

These results indicate that the disproportionation behavior of $(C_4H_4)_2Fe_2(CO)_n$ is very similar to that of $(C_5H_5)_2Mn_2(CO)_n$. Thus $(C_4H_4)_2Fe_2(CO)_3$ is stable with respect to such disproportionation to $(C_4H_4)_2Fe_2(CO)_4$ + $(C_4H_4)_2Fe_2(CO)_2$, which is consistent with its relatively high CO dissociation energy (Table 14). However, the disproportionation of $(C_4H_4)_2Fe_2(CO)_4$ into $(C_4H_4)_2Fe_2(CO)_5$ + $(C_4H_4)_2Fe_2(CO)_3$ is exothermic (Table 14), suggesting that in the $(C_4H_4)_2Fe_2(CO)_n$ system the Fe═Fe double bond is unstable with respect to the Fe−Fe single bond + the Fe≡Fe triple bond. The related disproportionation of $(C_5H_5)_2Cr_2(CO)_5$ with a Cr═Cr double bond into $(C_5H_5)_2Cr_2(CO)_6$ with a Cr−Cr single bond + $(C_5H_5)_2Cr_2(CO)_4$ with a Cr≡Cr triple bond has been observed experimentally.[16]

4. Summary

The results from our DFT studies on the binuclear cyclobutadieneiron carbonyl derivatives $(C_4H_4)_2Fe_2(CO)_n$ may be summarized as follows. Only one low-energy structure is

predicted for the pentacarbonyl, namely, $(\eta^4\text{-}C_4H_4)_2Fe_2(CO)_4(\mu\text{-}CO)$ with an Fe−Fe single bond (2.743 Å by BP86) and a single bridging CO group. Both singlet and triplet doubly bridged structures $(\eta^4\text{-}C_4H_4)_2Fe_2(CO)_2(\mu\text{-}CO)_2$ are found for the tetracarbonyl. The triplet structures have either ~2.6 Å Fe−Fe distances, suggesting single bonds with 17-electron iron configurations, or with ~2.4 Å Fe═Fe distances, suggesting double bonds with 18-electron iron configurations. In the latter case the Fe═Fe bond is a $\sigma + {}^2/_2\pi$ bond similar to the O═O bond in triplet dioxygen. For the tricarbonyl the experimentally known[12,13] singlet triply CO-bridged structure $(\eta^4\text{-}C_4H_4)_2Fe_2(\mu\text{-}CO)_3$ with an Fe≡Fe triple bond (2.15 Å) is found as well as a higher energy doubly bridged triplet structure $(\eta^4\text{-}C_4H_4)_2Fe_2(CO)(\mu\text{-}CO)_2$. For the dicarbonyl and monocarbonyl both coaxial and higher energy perpendicular structures are found. The triplet coaxial structure $(\eta^4\text{-}C_4H_4)_2Fe_2(\mu\text{-}CO)_2$ with an Fe≡Fe triple bond is of lower energy than the corresponding singlet structure, which would require an Fe−Fe quadruple bond to give the iron atoms the favored 18-electron configuration. The singlet, triplet, and quintet coaxial structures for the monocarbonyl have four-electron donor bridging $\eta^2\text{-}\mu\text{-}CO$, as indicated by unusually low $\nu(CO)$ frequencies around 1600 ± 20 cm^{-1}.

These results lead to the following general observations on the $(C_4H_4)_2Fe_2(CO)_n$ systems:

(1) Structures with Fe═Fe double bonds are relatively unfavorable, as indicated by the predicted exothermic disproportionation of $(C_4H_4)_2Fe_2(CO)_4$ into $(C_4H_4)_2Fe_2(CO)_5 + (C_4H_4)_2Fe_2(CO)_3$ as well as the existence of separate triplet $(C_4H_4)_2Fe_2(CO)_4$ stationary points of similar energies with Fe−Fe single σ bonds and Fe═Fe double $\sigma + {}^2/_2\pi$ bonds.

(2) Structures with Fe−Fe quadruple bonds are also not favorable since triplet $(C_4H_4)_2Fe_2(\mu\text{-}CO)_2$ with an Fe≡Fe triple bond is of lower energy than singlet $(C_4H_4)_2Fe_2(\mu\text{-}CO)_2$; the latter structure is required to have a Fe−Fe quadruple bond for the favored 18-electron configuration.

(3) The extreme electron deficiency/coordinative unsaturation of $(C_4H_4)_2Fe_2(CO)$ is partially balanced by four-electron donor bridging $\eta^2\text{-}\mu\text{-}CO$ groups in the lowest energy singlet, triplet, and quintet structures.

(4) Perpendicular structures of the highly unsaturated $(C_4H_4)_2Fe_2(CO)_2$ and $(C_4H_4)_2Fe_2(CO)$ are possible, but are of higher energy than the corresponding coaxial structures.

Acknowledgment. We are grateful to the China National Science Foundation (Grant 10774104) and the U.S. National Science Foundation (Grants CHE-0209857, CHE-0451445, and CHE-0716718) for support of this work.

Supporting Information Available: Complete tables of vibrational frequencies for $(C_4H_4)_2Fe_2(CO)_n$ ($n = 5, 4, 3, 2, 1$) structures (Tables S1 to S23); complete Gaussian reference (ref 33). This material is available free of charge via the Internet at http://pubs.acs.org.

OM701246H